Hindawi
Journal of Engineering
Volume 2023, Article ID 1426506, 12 pages
https://doi.org/10.1155/2023/1426506

Research Article

Design and Realization of a Controlled Electromagnetic Breaking System

Tchahou Tchendjeu Achille Ecladore, Yungho Edickson Bobo, and Nfah Eustace Mbaka

Electrical and Electronic Engineering Department, National Higher Polytechnic Institute, The University of Bamenda, Bambili, Cameroon

Correspondence should be addressed to Tchahou Tchendjeu Achille Ecladore; tchahoutchendjeu@gmail.com

Received 20 April 2023; Revised 12 July 2023; Accepted 27 July 2023; Published 14 August 2023

Academic Editor: Paolo Castaldo

Industrial machines with sharp moving blades are extremely dangerous to workers. These machines often rotate for some time (called the run-down time) before completely stopping due to little or no brakes. In the case where brakes are used, they are mechanical in nature and are associated with problems of wear out and frequent maintenance among others. In this paper, we proposed a mathematical model and implementation of an electromagnet and design and construction of a mechanical support frame and a controller for the electromagnetic braking system. The electromagnetic braking system works on the principle of electromagnetism. To realize the semicircular electromagnets, we coil the gauge wires several times around a ferromagnetic core material. The electromagnet was connected to a 12 V 7 Ah battery and was used to lift a load whose mass and corresponding weight were predetermined using a scale balance. The magnetic force generated was equal to the amount of maximum load it could lift. The mechanical frame, on which the electromagnets, motor, battery, switches, and chain drive system were mounted, was designed using SolidWorks and constructed by measuring, cutting, and joining of iron materials. A microcontroller and a power MOSFET were used in the control circuit to drive the electromagnet. Major results such as the realized electromagnets and the magnitude of the electromagnetic force (1.43 N) produced by the electromagnets are presented. The mechanical frame and the control circuit are also presented. The braking force was greater than the rotation torque of the disc, and hence braking was achieved.

1. Introduction

In many processing industries such as brewing industries, food industries, wood industries, foundries, and other industries such as electromechanical, automotive, and others, there is a very rapid development rate thanks to the implementation of new technologies. These industries generally have rotating machinery which after the power cut continues to run for a long period called downtime. Due to the damage these rotating machines typically cause during downtime, it is often necessary to reduce the downtime of these machines. The braking technology in automobiles is based on the friction system which converts the kinetic energy of the body into thermal energy causing the movement to slow down. To stop the motion of a rotating body, the stopping force by the braking system must be greater than the actual energy generated by the motor system. There are also power-assisted braking systems that use hydraulic or pneumatic systems to apply the brakes. In the hydraulic braking system, the pedal is connected to the brake pads of each wheel by fluids or air. The incompressible fluids transmit the force through channels to the various wheels once the force is applied to the pedals. The hydraulic braking system is a complex system to build [1], it requires frequent maintenance, and any leak in the system leads to failure; all of these are the disadvantages of power-assisted braking systems. Another braking system is the electromagnetic brake. Electromagnetic brakes are mechanical brakes that cause retardation by applying electromagnetic induction in the disc brake in the opposite direction to the rotation of the actual disc. If a wheel moves clockwise, then

the magnetic field will be counterclockwise. Without physical contact, the movement of the wheels is retarded when the magnetic field is created [2]. When an object is in rotation or translation, the main role of the braking system is to cancel or reduce the speed of the object. A braking system can also be used to maintain the position of a moving object in its state. During braking, the brake absorbs kinetic energy and the drag force to stop the object is provided by friction; then, the absorbed energy is then transformed into heat [3]. Electromagnetic braking systems, also called eddy current brakes or magnetic brakes, slow down or stop movement by using magnetic force to apply mechanical torque in the form of resistance or friction. In the middle of the 20th century, with the appearance of trains and trams, the techniques for designing braking systems exploded, but the basic operating principle remained the same. Generally, magnetic brakes work with magnetic energy with the principle of magnetism. These systems operate on the basis of Faraday's law of electromagnetic induction and Lenz's law and are frictionless. Because magnetic brakes are frictionless brakes, they reduce the damage in the brakes. The electromagnetic braking system has been implemented to overcome the limitations and shortcomings of the traditional braking system. To slow down or brake the movement of industrial machinery, braking systems are also used. Most industrial machines with moving blades are sharp or have teeth filed with sharp materials that can vibrate or kick back. However, when you need to provide quick braking, the only thing that stands between a safe stop and disaster is the science of friction. Solving the downtime problem of a rotating machine requires designing an interlock linked to an automatic brake that eliminates or considerably reduces the downtime and also controls risks.

In this paper, we propose an electromagnetic braking system based on an electromagnet model for non-contact braking system. We have combined this electromagnetic braking system with a controller and a mechanical support frame. We offer the electromagnetic brake system with flux controlled mechanism because it proves to be more reliable than other brake systems. In the literature, it has been noted that electromagnetic brakes account for approximately 80% of all electrically controlled braking applications.

The rest of this piece of work is presented as follows. In Section 2, related works to our paper are presented. Section 3 presents the materials and methods to design and realize our proposed system, and in Section 4, we depict the results of our work followed by a discussion. Conclusion is presented in Section 5.

2. Related Works

Around the years 1786–1853, François Arago, after observing the phenomena of eddy currents [4], introduced the concept of an electromagnetic braking system. François Arago observed in 1824 rotary magnetism and found that most conductive materials can be magnetized. The discoveries we have just indicated were completed and explained by Michael Faraday (1791–1867). Heinrich Lenz stated Lenz's law in 1834, namely, the direction of the induced current flowing in an object will be such that its magnetic field will oppose the change in magnetic flux which caused the current flow. French physicist Léon Foucault (1819–1868) is credited with discovering eddy currents. It has been found that eddy currents produce a secondary field which cancels part of the external field and causes part of the external flux to avoid the conductor. Léon Foucault in September 1855 discovered that the force necessary for the rotation of a copper disc becomes greater when it is rotated with its rim between the poles of a magnet, the disc being heated at the same time by the eddy current induced in the metal. In 1879, David E. used eddy currents for non-destructive testing. This principle has also been used to carry out metallurgical sorting tests. After these tests were carried out, studies were carried out by researchers to understand the principle of operation of eddy currents in order to use them in most industrial applications such as vehicles, trains, and planes. The research carried out in this direction has led to the publication of books and articles. Some research results will be presented in the following. According to reference [5], to engage a brake, the magnetic force of an electromagnetic braking system can be used with the power required for braking transmitted manually. In this case, the brake disc is connected to a shaft and the electromagnet is mounted on the frame. Once electric current flows through the coil of the electromagnet, a magnetic field develops across the armature due to the current flowing through the coil and causes the armature to attract towards the coil. This phenomenon produces and develops a torque, and the vehicle comes to a standstill. The authors in [6] indicate that most braking systems use frictional forces to transform the kinetic energy of a moving body into heat which is dissipated by the brake pads. In friction braking systems, overuse of the brake causes the temperature of the brake pads to rise, reducing the effectiveness of the system. Yet in an electromagnetic braking system, the braking disc is connected to a shaft and the electromagnet is mounted on the frame; when electricity is applied to the coil, a magnetic field develops across the armature which creates the eddy current. This current induces the reverse magnetic field and causes the motion to decelerate. Some authors in [7] proposed an automatic braking system for an electric motor vehicle, linked to the motor for the transmission of the movement of the motor to a brake lever which pushes the restraint. Mechanical handbrake devices still known as brake by wire are increasingly being replaced by typical parking brake systems by a system of electrical parts. This is possible by replacing the typical linkages with electric motor units. Braking force is generated directly at each wheel by high-performance electric motors and automotive management, this unit being controlled by an electronic control unit (ECU). Nowadays, the electronic parking brake replaces the traditional parking brake with a switch in the center console of the automobile. The handbrake of the mechanical device offers the following advantages over the traditional handbrake: the ease of use of the handbrake is fully applied, regardless of the strength of the driving force. The electric safety handbrake applies mechanically once the key is removed from the ignition. In their analysis, the authors in [8] showed that the eddy current brake is one of the most remarkable principles of the electromagnetic induction phenomenon; even though it seems to

have many technical problems due to the dissipative nature, it has some valuable contributions. The main objective in that paper was to achieve efficient braking performance without any physical contact, and its only solution to overcome this problem is a conventional integrated eddy current braking system. The research of that paper has concluded that if integrated eddy current brakes are used in automobiles, braking efficiency increases compared to the current friction brake which can result in the reduction of braking cost in automobiles to a large extent. The authors of [9] conducted a study to see how to increase the braking torque of an electromagnetic braking system. In their studies, they found that the greater the thickness of the disk, the greater the number of turns of the electromagnet and the greater the electrical conductivity of the conductor, which results in the production of a greater braking torque. The permanent magnet eddy current brake uses neodymium-iron-boron (NdFeB) magnets. The eddy current analysis of permanent magnets shows that the parallel magnetized eddy current topology has the superior braking torque capability. In an electrically controlled eddy current braking system subjected to time-varying fields with different waveforms, the application of the triangular wave field results in the highest braking torque. It was also found that the electromagnetic brakes interfered with the signaling and train control system. Permanent magnet eddy current brakes are a simple and reliable alternative to mechanical or electromagnetic brakes in transportation applications. The greater the speed, the greater the effectiveness of eddy current braking. Therefore, the authors also worked on the development of permanent magnet eddy current braking system. Their discoveries are important because they allow us to know how to increase the braking torque by improving the number of turns of the coils and the type of magnets to be used. The authors of [10] worked on the progress of electric vehicles using eddy current brakes. They discovered that the force derived from this brake would be directly proportional to the speed of the rotor. The brake would slow down but never stop. They decided to set up an eddy current braking system integrated into the motor so that once the brake became ineffective, the motor could stop the vehicle.

3. Materials and Methods

To build an electromagnet, the copper wire is wound on the semicircular body of a ferromagnetic material. The model of electromagnet that we offer is built and fixed on the side of the rotating wheel. Our electromagnet is mounted on a metal support and is powered from a 12 V direct current power supply connected in series with a power electronics switch. We used a microcontroller to generate a PWM signal to control a MOSFET. This transistor along with the control signal controls the current that flows through our electromagnet. We added a DC motor on the metal support that we also powered at 12 V. This motor, when powered, transmits the kinetic energy of rotation to a pulley through a chain.

3.1. Braking Principle of Operation. When a disc made of conductive material is held rotating at high speed in a magnetic flux and intersects the magnetic field lines, an electromotive force (emf) is produced in this disc by the law of electromagnetic induction proposed by Faraday. The birth of the electromotive force causes the formation of eddy currents in this disc as shown in Figure 1. The eddy currents generated in the disc circulate in the form of loops. Due to the law of self-induction, these eddy currents independently produce a magnetic field which is in the opposite direction to the magnetic field of the source. The birth of a magnetic field opposite to that which gives rise to it generates a drag force which converts the kinetic energy of rotation into thermal energy. This drag force is the braking force, and it is proportional to the change in the magnetic field, the strength of the magnetic flux, and the rate of change at which the disc is cut. In the electromagnet, an excitation coil creates a magnetic field by current flow. This coil develops lines of magnetic flux between the metal discs, thereby attracting the armature to the face of the metal disc. In the event that the current is diminished or removed, the metal disk is free to rotate. This shows that by controlling the power supply of the coil, we control the drag force or even the rotational movement in the wheels. With this type of braking, slippage is observed during deceleration when the brake is engaged. Once the brake has fully stopped, the slipping disappears.

3.2. Braking System Functioning Principle. The proposed system is divided into two parts: the experimental setup component and the braking component, as presented in Figure 2.

In the diagram of Figure 2, there is an electric motor which converts electrical energy into mechanical energy. This energy is transmitted to the wheel by a chain. The rotating wheel under test is a blade that will move under a magnetic flux. When a magnetic field is produced, the wheel under test will experience a slowdown in speed. The electrical power supply shown in the diagram allows the supply of electrical energy to the experimental setup and to the magnetic field production circuit. The function of the regulator is to regulate the electrical energy supplied to the control circuit. The microcontroller is the controller that produces a pulse-width modulation (PWM) signal needed to control the magnetic field produced. The power MOSFET is the interface between the microcontroller and the electromagnet. The current produced by the microcontroller is quite low and cannot produce the current needed to operate the electromagnet. The use of the MOSFET makes it possible to amplify the control current to produce the necessary magnetic field. The electromagnet is a set of coils constructed to behave like a magnet when energized which will create a concentrated magnetic field at the edge of the moving blade. The concentrated magnetic field at the edge of the moving blade creates an eddy current, and the eddy current produces an electromagnetic force opposing the rotation of the blade which in turn slows down the speed and eventually may even stop.

3.3. Materials. During the design of electromagnetic brakes, the selection of materials is an essential part of this process. The materials used in the electromagnetic braking system

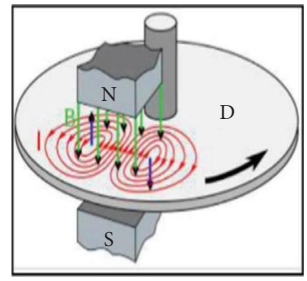

Figure 1: Principle of eddy current [11].

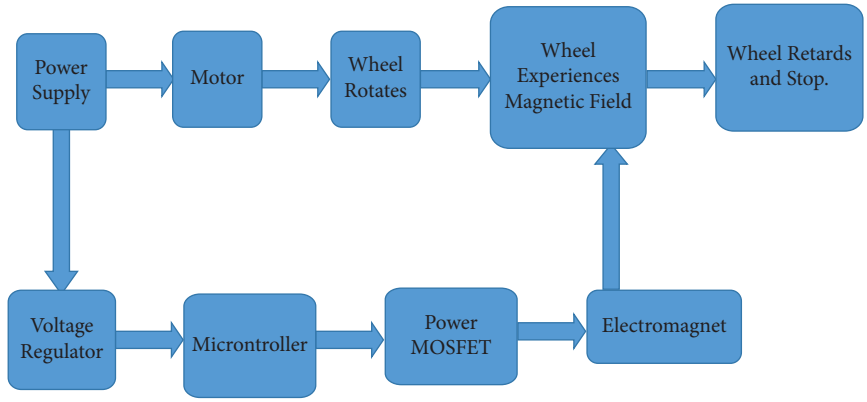

Figure 2: Proposed braking system block diagram.

have a crucial influence on the magnetic circuit as well as the structural and thermal characteristics. Here, the issue of material selection is discussed in terms of magnetic, structural, and thermal properties. However, it is good that we first start by presenting the materials necessary for the construction of the project. Manufacturing materials are both software and hardware. We used SolidWorks to design the mechanical support frame. The hardware components used in this work are DC motor, chain belt, wheels, metal disc, electromagnets, control switch, fasteners or bearings, shaft, pulley, battery, iron bars, nuts or bolts, cables, gauge coils, lighter gas, welding machine, welding electrodes, gum paper tape, and connectors.

In order to keep the wheel moving, a rotating source is needed. The DC motor transmits the rotational motion to the wheel. The electric motor converts electrical energy into mechanical energy by electromagnetic induction. Here we used the typical 12 volt grinder motor with a rated speed of 600 RPM and a rated power of 30 watts.

To transmit power from the engine to the wheel's rotating shafts, we used a V-520 chain with internal width belts between plates of 6.35 mm. The total width of the selected chain is 21.5 mm.

The chosen metal is a ferromagnetic material that responds to magnetic properties. Considering the cost, permeability, and availability, low-carbon steel, AI 6061, is selected as the ferromagnetic material in the magnetic circuit. Additionally, AI 6061 has a high yield strength.

The electromagnet is an element of the system we propose, and we manufactured it based on the calculations, sizing, and careful choice of the following parameters: the amount of current, the required voltage of the power supply, the size of the wire of gauge which can bear the rated current, and the number of turns which can supply the sufficient magnetic force. In the methodology part of this paper, more information is given.

The circuit board is an important component of the system. It is the part of our system that electrically connects the mechanical components to perform the control action. The circuit is composed of a field effect transistor (MOSFET), a regulator, and a microcontroller mounted on an Arduino board. The MOSFET switch is used to control the power supply to the electromagnet as mentioned above. The electromagnet is also connected to it. Also, on the circuit board is a typical common electrical switch. When the rotation of the pulley needs to be stopped, the braking is applied by activating the switch. When free rotation of the pulley is required, the switch is deactivated. The regulator controls and regulates the voltage and power supplied to the circuit or the amount of voltage supplied to the electromagnet. Thus, the power sources in a circuit may have fluctuations that do not provide a fixed output voltage. The built-in voltage regulator maintains the output voltage at a constant value. The microcontroller is used to produce a pulse-width modulation signal to control the braking force generated by the electromagnet.

To fix the motor and the electromagnet on the mechanical support as well as the metal disc with the pulley, bolts and nuts are used. M7 × 1 mm bolts (i.e., 7 mm in diameter and 1 mm thread) and M13 × 1.5 mm nuts are used for joints with a wooden base. M4 × 1 mm bolts and M8 × 1 mm nuts are used to assemble the disc with the pulley.

To transmit and vary the rotational movement of the various parts of the system, a shaft of conical sizes of 2 × 55 mm and 2 × 25 mm and a thread diameter of 14 mm was selected. The material of the shaft is suitable iron, and the diameter is adjusted according to the inner diameter of the wheel.

We have selected deep groove ball bearings because of their ability to be used in axial and radial loads. Here we have selected a 6005 series parameter bearing, with 25 mm inner diameter, 47 mm outer diameter, and 12 mm width.

The motor and electromagnet are run on a 12 v supply. To provide the rated voltage in this project, a 12 V 7 Ah DC battery was selected to power the system. A twelve volt battery has six single cells in series producing a fully charged output voltage of 12.6 volts.

The frame is the structural part of the system that supports the components of the physical construction such as the axles, the wheel, the clamps connecting the electromagnet, and the circuit board support. The vertical steel columns and horizontal beams are constructed in a rectangular grid that balances even the vibration produced by wheel movement and even has the ability to handle the stopping force of the wheel by the electromagnets.

3.4. Design Methodology. To design a model, everything starts with a systematic plan where the manufacturing is subdivided into seven stages. The different steps are as follows: (1) analyze the design elements—here we collect all relevant data about the problem; (2) identify the characteristics of the electromagnetic brake capable of overcoming the problem; (3) analyze the electromagnetic braking system—here we analyze the system focusing on the principle of operation and the manufacturing materials required for the model to be made; (4) sizing the electromagnetic braking system—in this step, we are more focused on the calculation of the constraints of the components to be used to manufacture the brake according to the starting specificities and the choice of the components according to the standardized values; (5) manufacture the model according to the specifications given and check if the mechanisms work perfectly; (6) test—the model is tested to check if it meets the initial requirements; once the test is completed, we proceed with the implementation of the model; and (7) result—the measurements taken are displayed in the form of a table and certain results are deduced from the measurements obtained by carrying out some calculations.

We can identify four basic parameters useful in sizing an electromagnet. Varying any of the four basic elements of an electromagnet allows us to tune the field strength to your needs. One way to increase or decrease the strength of the magnetic field is to change the number of loops in the coil. Generally, the mathematical relation between the number of loops N and the magnetic field B is a relation of proportionality. Changing the metal core to a different metal will make the electromagnet stronger or weaker as the magnetic field varies depending on the metal core. Steel cores create weaker fields. Neodymium cores create the strongest field. Although metal wires are very efficient conductors of electricity, they have some resistance to current flow. The use of conductive wires with a large section to make the coil will reduce the electrical resistance of the electromagnet. This has the advantage of increasing the current and therefore the magnetic field. Using smaller gauges will increase resistance. This results in the reduction of the current and therefore the weakening of the magnetic field. In electromagnetism, permeability is the measure of the magnetization that a material obtains in response to an applied magnetic field. According to Ampère's law, the magnetic field around a current-carrying wire is directly proportional to the intensity of the current. The approach to producing the braking torque is to use the amount of braking force multiplied by the eddy current braking radius. Due to the braking force and electromagnetic interactions, the amount of braking force can be calculated using the Lorentz force. The magnitude of the force is calculated as shown in equation (1), from the magnitude of the magnetic field and the current flowing in a certain volume.

$$\overrightarrow{F_d} = \iiint \overrightarrow{J}\,\overrightarrow{B}\,\mathrm{d}V, \tag{1}$$

where $\overrightarrow{F_d}$ is the electromagnetic force, $\overrightarrow{J}$ is the current density, $\overrightarrow{B}$ is the magnetic field, and dV is the elementary volume through which the current flows.

The amount of braking torque is calculated using the following equation:

$$T_d = \iint r_p\,(JB)\mathrm{d}S, \tag{2}$$

where r_p is the radius of the blade.

Following the shape and the magnetic circuit of the breaking system depicted by Figure 3, the electromagnetic force can be calculated using the following equation:

$$F = \frac{AB^2}{2\mu_0}, \tag{3}$$

where A is the area of the blade and μ_0 is the permeability of air.

The power of the electromagnet which is manually constructed can be calculated using the following equation:

$$F = \frac{\mu_0 A\,(\mathrm{NI})^2}{2G}, \tag{4}$$

where N is the number of turns in the electromagnetic core, I is the current circulating in the coil, and G is the air gap between the electromagnet and the blade.

The shape of the magnetic core is designed according to the circular shape of the rotating metal disc. With this in mind, two electromagnets of circular shape and of identical material at the level of the core were built. Each

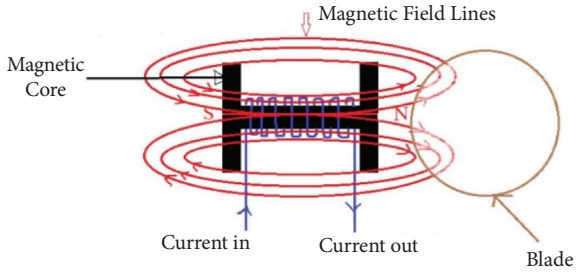

Figure 3: Magnetic circuit of the braking system.

electromagnet is made up of an inner core which is a straight iron measuring 2 cm in length and 1.5 cm in width. The core width is the same as the core diameter. To guide the winding coils on the core, the outermost part was designed in a semicircular fashion with the following dimensions: radius of the electromagnet, $r = 7$ cm, and the height of the electromagnet, $d = 14$ cm.

The insulation of the magnetic core is a very essential factor in the manufacture of the electromagnet. Insulation of the magnetic core helps to prevent the entire electromagnet from short circuit currents, increasing the force generated by the electromagnets and thus reducing the temperature of the heating coils. Based on the gauge current capabilities from Table 1, we selected a wire. This gauge wire is capable of carrying the current produced by the battery source. Two wires of different gauge are used to produce the electromagnets. Each of the coils has its own diameter, its own resistance per meter, and its own current-carrying capacity.

Considering a 12 v power supply, our input voltage to the copper wire is 12 v DC. From Table 1, we can get the maximum current that the copper wire can carry. Therefore, using Ohm's law from equation (5), we can determine the total cable resistance for a safe design.

$$R = \frac{V}{I}, \tag{5}$$

where V is the applied voltage across the gauge wire, I is the current through the gauge wire, and R is the total resistance of the gauge wire.

For the case of gauge wire 17, $I_{\max} = 4.7\,A$ and $V = 12V$. Using equation (5), we have $R = 2.55\,\Omega$. From Table 1, it can be seen that the resistance at 100 m is 1.35, for a resistance of 2.55 Ω, and then the minimum length of 17 gauge wire is 189 m. For this dimensioning, we choose $L = 200$ m. The diameter of 17 gauge wire is $d = 1.2$ mm, so the cross section of 17 gauge is 1.58 mm^2. For the case of 20 gauge wire, I_max = 1.8 A and $V = 12$ V. Using equation (5), we have $R = 6.67\,\Omega$. From Table 1, it can be seen that the resistance at 100 m is 3.4, of a resistance of 6.67 Ω, so the minimum length of 20 gauge wire is 196 m. For this dimensioning, we choose $L = 200$ m. The diameter of this 20 gauge wire is $d = 0.914$ mm, so the cross section of the 20 gauge is 0.66 mm^2. Considering the core sizes given above and the fact that the height of the core is 5 cm, the average rotation ratio is therefore 0.667. From this value, the calculation of the total number of turns $N = 300$. We choose $N = 350$ turns for the two gauge coils.

Table 1: Gauge wire chart [12].

AWG	Dia (mm)	SWG	Dia (mm)	Max amps	Ohms/100 m
11	2.30	13	2.34	12	0.53
12	2.05	14	2.03	9.3	0.67
13	1.83	15	1.83	7.4	0.85
14	1.63	16	1.63	5.9	1.07
15	1.45	17	1.42	4.7	1.35
16	1.29	18	1.219	3.7	1.70
18	1.024	19	1.016	2.3	2.7
19	0.912	20	0.914	1.8	3.4
20	0.812	21	0.813	1.5	4.3
21	0.723	22	0.711	1.2	5.4
22	0.644	23	0.610	0.92	6.9
23	0.573	24	0.559	0.729	8.6
24	0.511	25	0.508	0.577	10.9
25	0.455	26	0.457	0.457	13.7
26	0.405	27	0.417	0.361	17.4
27	0.361	28	0.376	0.288	21.8
28	0.321	30	0.315	0.226	27.6
29	0.286	32	0.274	0.182	34.4
30	0.255	33	0.254	0.142	43.9
31	0.226	34	0.234	0.113	55.4
32	0.203	36	0.193	0.091	68.5
33	0.180	37	0.173	0.072	87.0
34	0.160	38	0.152	0.056	110.5
35	0.142	39	0.132	0.044	139.8

From Table 1, it can be seen that the resistance at 100 m is 1.35, for a resistance of 2.55 Ω, and then the minimum length of 17 gauge wire is 189 m. For this dimensioning, we choose $L = 200$ m. The diameter of 17 gauge wire is $d = 1.2$ mm, so the cross section of 17 gauge is 1.58 mm^2. For the case of 20 gauge wire, I_max = 1.8 A and $V = 12$ V. Using equation (5), we have $R = 6.67\,\Omega$. From Table 1, it can be seen that the resistance at 100 m is 3.4, of a resistance of 6.67 Ω, so the minimum length of 20 gauge wire is 196 m. For this dimensioning, we choose $L = 200$ m. The diameter of this 20 gauge wire is $d = 0.914$ mm, so the cross section of the 20 gauge is 0.66 mm^2. Considering the core sizes given above and the fact that the height of the core is 5 cm, the average rotation ratio is therefore 0.667. From this value, the calculation of the total number of turns $N = 300$. We choose $N = 350$ turns for the two gauge coils.

The mechanical design and construction of the frame is an important part of this article. In order to use computer-aided design to model the proposed system, we used the SolidWorks 2018 version and the sketch environment. A series of lines of lengths 72 cm, 20.5 cm, and 20 cm corresponding, respectively, to the length, width, and height of the frame have been drawn. We used welding so as to come out with a solid model of the frame. Blue color paint was added to the frame, and two circles of diameter 65 cm and 12 cm were drawn, the boss extrusion and extrusion cutter function were used to output the solid model of the steering wheel, and finally an aluminum material was then applied to the steering wheel. For the gables, two circles of diameter 6.5 cm and 12 cm were drawn, and the boss extrusion and extrusion cut function were used to output a solid model of the gables, and finally, an aluminum material was then applied to the

small and large gables. The 20 mm length chain link sketch was first drawn using line, circle, arc, and cut tools in a sketch environment to generate the solid model chain. A tire section profile with a width of 5.5 cm and a height of 4.5 cm was drawn in a sketch environment for a bicycle tire, using the base function of revolution, a tire with a diameter of 35 cm was generated, an anchor pattern was then created on the tire using the pattern tool, and finally rubber was applied to the tire. A circle 35 cm in diameter was drawn in the sketch environment for the tire rim, this circle was then offset by an offset distance of 1 cm using the offset tool, the contour of the sketch was then extruded to a distance of 3.2 cm using the extrude boss feature, the extrude feature was used to create a concave groove on the rim and then a line of 17.5 cm was drawn on the rim, and finally an aluminum material was then applied to the rim. Finally, a 0.7 HP motor was imported and other items were added to assemble and come out with the whole design model. To achieve our mechanical design, we cut four pieces of mild steel 20 cm high, two pieces 72 cm long, and two other pieces 20.5 cm wide, all of the same thickness of 4 mm. These parts were assembled by arc welding to form a rectangular mechanical frame. In addition, two other mild steel supports 18 cm high and 2 mm thick were cut. These support bars were connected to the mechanical base frame 17 cm from one end of its length. Between these two steels we inserted the shaft attached on both sides with M13 × 1.5 mm nuts. On this shaft, we mounted the pinion, the bearing, the metal disc, and the wheel containing the tire. On the side containing the metal disc, we placed our electromagnets on one of the supports. Based on our chain length and required tension, we placed the motor at the other end of the mechanical frame using M7 × 1 mm bolts and nuts. On the motor shaft, we tied a sprocket to which the chain was attached. A 15 × 15 cm extension plate was attached to the center of the frame length to carry the battery and control circuitry. The entire frame was then lined with a white oil paint.

The materials used in the construction of the mechanical frame are iron bars, bolts, and nuts. The following dimensions were selected to build the mechanical frame: width $w = 20.5$ cm, length $l = 72$ cm, and height $h = 20$ cm. The iron bars were measured and cut according to the dimension indicated above. They were assembled using the welding electrodes. Bolts and nuts were used to attach some parts that did not require welding. We considered the maximum load on the frame (battery, electromagnet, motor, pulley or wheel, and chain drive) at $m = 15$ kg. With this, the bending moment of the frame is $M = 10584$ Nmm, calculated using the following equation:

$$M = \text{mgl}, \tag{6}$$

where m is the mass of load on the frame, g is the gravity, and l is the length of the frame.

Another important parameter to be determined is the stress on the frame. Using the relation in equation (7), the stress can be determined.

$$\frac{M}{I} = \frac{\sigma}{Y}, \tag{7}$$

where M is the bending moment, I is the moment of inertia about the bending axis, σ is the stress, and Y is the distance of the layer at which the bending stress is considered.

According to the shape of the frame, the moment of inertia about the bending axis is obtained using the following equation:

$$I = \frac{lh^3}{12}. \tag{8}$$

From equations (7) and (8), the stress of the frame is $\sigma = 13.23$ MPa. According to the material used to construct the frame, the allowable shear stress is calculated using the following equation:

$$\sigma_{\text{all}} = \frac{\text{Syt}}{\text{Fos}}, \tag{9}$$

with Syt, the yield stress, being 210 MPa and Fos, the safety factor, being 2. Therefore, the allowable stress is 105 MPa. We can notice that $\sigma < \sigma_{\text{all}}$.

A shaft is the component of a mechanical device that transmits rotational motion and power from one rotating point to another. It is integral to any mechanical system in which power is transmitted from a prime mover, such as an electric motor or another engine, to other rotating parts of the system. The diameter of the shaft is determined using the following equation:

$$\frac{T}{J} = \frac{\tau}{r_S}, \tag{10}$$

where T is the twisting moment, J is the moment of inertia, τ is the torque on the shaft, and r_S is the radius of the shaft. The moment of inertia of a round solid shaft is calculated using equation (11), where d_S is the diameter of the shaft.

$$J = \frac{\pi d_S^4}{32}. \tag{11}$$

From equations (10) and (11), the diameter of the shaft is calculated using equation (12). Using the torque produced by the motor, the diameter of the shaft is $d_S = 15$ mm. Considering the safety factor and normalized values, the diameter of the shaft is chosen to be $d_S = 40$ mm.

$$d_S = \sqrt[3]{\frac{16T}{\pi\tau}}. \tag{12}$$

The rotational motion of the motor is to be transmitted to the main pulley shaft by contact. The motion of the main pulley shaft is transmitted to the pulley of the wheel through a chain. For that reason, we have to calculate the rotational speed of the wheel, the torque, and the stress developed at the wheel shaft. The diameter of the main pulley shaft and motor shaft is chosen to be 60 mm and 40 mm, respectively. The nominal speed of the motor is chosen to be 600 rpm. Using equation (12), the rotational speed of the main pulley shaft is 400 rpm.

$$\frac{N_1}{N_2} = \frac{D_2}{D_1}, \tag{13}$$

where N_1 is the rotational speed of the motor, N_2 is the rotational speed of the main pulley, D_1 is the diameter of the main pulley shaft, and D_2 is the diameter of the motor shaft. By using the same equation (12), we have determined the rotational speed of the wheel to be 83 rpm knowing that the diameter of the shaft of the wheel is 290 mm. To calculate the torque developed at the wheel shaft, we started by calculating the torque developed at the main pulley shaft using equation (13). The power developed by the motor is chosen to be 30 W; considering that the power of the motor is transmitted to the pulley shaft and knowing the rotational speed of the main pulley, the torque developed on the pulley shaft is 716 Nm and the induced stress on the pulley shaft is 0.253 MPa using equation (7). Using the same data and equations, we found the torque developed at the shaft wheel to be 3462 Nm and the stress on the wheel shaft to be 0.052 MPa. We can notice that the stress on the main pulley shaft and wheel shaft is far smaller than the allowable value which is 105 MPa.

$$P = T\omega, \tag{14}$$

where P is the power developed by the motor, T is the torque, and ω is the angular speed of the motor.

Another element we have to size is the chain. The calculation using equation (14) yields that the length of the chain is 1 m.

$$L = \frac{(16 + 8\pi)(D_1 + D_3)^2}{2 + (D_1 - D_3)}. \tag{15}$$

Braking is not an instantaneous process. For us to achieve this, we need to control the growth of current across the terminals of the electromagnet. We designed and implemented a controller circuit in Proteus to regulate the current flowing into the electromagnet to control the breaking time. This circuit consists of an Arduino microcontroller that executes a program which enables the generation of the required control signal. A metal-oxide-semiconductorfield-effect transistor (MOSFET) is used as an interface to drive the brakes. A flywheel diode is connected across the electromagnet to protect the MOSFET. A resistor of 10 k ohms called a pull-down resistor is connected between the push button and the ground to turn ON/OFF the microcontroller. The diagram of the control circuit drawn in the proteus environment is presented in Figure 4. Based on the braking criteria that require a systematic increase in the magnitude of the braking force, a pulse-width modulation code is written in Arduino Integrated Development Environment (IDE) and uploaded into the microcontroller of the Arduino Uno board. The pulse-width modulation (PWM) signal generated is sent to drive the MOSFET. The flowchart of the algorithm of the PWM generator is presented in Figure 5. When the motor is turned off, a breaking signal is sent to the microcontroller. Once the microcontroller receives the signal, an increasing voltage signal is generated every 1000 ms as presented in Table 2. In a period of 5000 ms, the voltage increases from zero volts to five volts, which enable the maximum

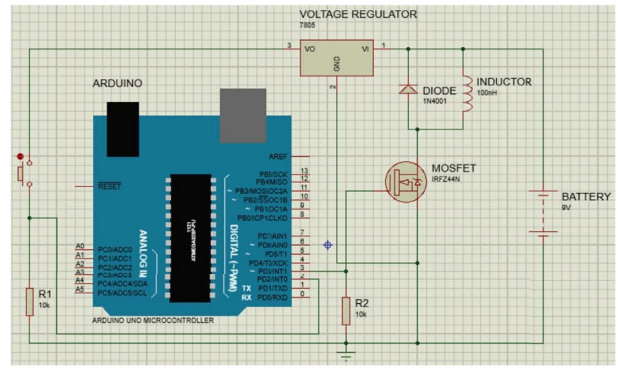

Figure 4: Electromagnet control diagram.

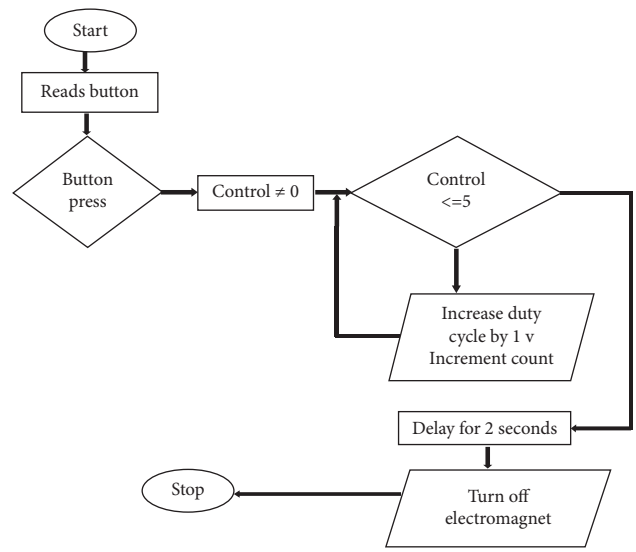

Figure 5: Flowchart of the PWM code.

current to flow into the electromagnet. Since the voltage is directly proportional to the force, this means that an increase in voltage leads to an increase in braking force. This magnetomotive force developed by the electromagnets grows with the braking time force. Using equation (14), the drain current of the MOSFET is calculated from the values of Table 2 and presented Table 3.

4. Results and Discussion

In relation to the stated requirements and the scope of designing, analyzing, realizing, and testing, the following results are presented for the controlled electromagnetic braking system.

$$I_D = k_n\left(\frac{W}{L}\right)[V_{GS} - V_{TH}]V_{DS}. \tag{16}$$

4.1. Results of the Electromagnet Fabrication. Figure 6 depicts the results of electromagnet realization. Figure 6(a) shows the top view and Figure 6(b) shows the front view of the magnetic core image after fabrication. Figure 6(c) shows the magnetic core realized with the gum paper applied to isolate

Table 2: Variation of the braking voltage with time.

Voltage (v)	1	2	3	4	5
Time (ms)	1000	2000	3000	4000	5000

Table 3: Characteristics of the drain source voltage and drain current.

V_{GS}	0	1	2	3	4	5
I_D	0	0.0158	0.032	0.047	0.063	0.078

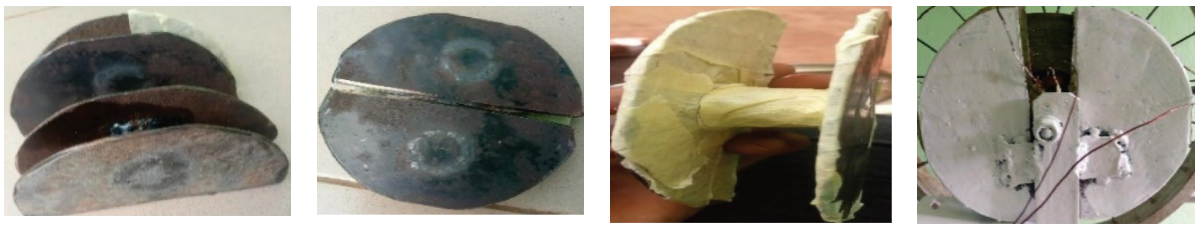

(a) (b) (c) (d)

Figure 6: Electromagnet realization: (a) top view of the magnetic core, (b) magnetic core front view, (c) gum paper tape insulation of the core, and (d) mounted electromagnet.

the core from the wire. Figure 6(d) shows the complete electromagnet made of the core and the wire mounted on the mechanical frame.

4.2. Results of the Mechanical Support Fabrication. Figure 7 depicts the results of the mechanical frame design. Figure 7(a) shows the result of the computer-aided design of the mechanical frame and the components of our proposed system using SolidWorks. Figure 7(b) shows the constructed mechanical frame and the other components of the proposed system mounted.

4.3. Results of the Electromagnet Controller. Based on the required current needed to flow into the coils of the electromagnet, we chose the MOSFET IRF44N. A voltage regulator LM7805 is chosen to supply the Arduino Uno board. From Figure 4, we can see that the drain current is the current flowing through the electromagnet. With the help of equation (4) and the current $I_{D,}$ we determine the electromagnetic force as presented in Table 4.

Using MATLAB software package, we plotted the data obtained in Tables 3 and 4. The graphical variations are presented in Figures 8 and 9, respectively. Figure 8 depicts the simulation result of the drain current versus the gate voltage of the MOSFET. We can notice that the drain current is proportional to the gate voltage. Figure 9 shows the simulation result of the breaking force versus the drain current. We can notice that as the drain current increases, the breaking also increases. This suggests that the breaking can be controlled through the gate voltage.

Figure 10 depicts the top view of the complete realized proposed system. On the image, we can see the motor and the motion transmission system, the battery, the mechanical frame, and the electromagnet. Figure 11 shows the simulation result of the drain current controlled by the microcontroller of the Arduino board.

Table 4: Electromagnetic force in function of drain current.

I_D	0	0.015	0.032	0.047	0.063	0.078
Force	0	0.136	0.622	1.343	2.41	3.699

4.4. Discussion. We designed and realized an electromagnetic braking system, with the main emphasis being laid at the level of the electromagnets. This electromagnetic braking system helps to solve the shortcomings of the traditional brakes, such as wear, brake fade, high heat generation, and frequent maintenance. Various designs, calculations, analyses, and observations were made to see how effective or efficient the system would be. Moreover, the electromagnet and the motor consume the energy supplied by the 12 v power supply. We know that the power of the motor is 30 W. This power together with the speed of the motor helps us to determine its rotational torque. Assuming transmission along the chain drive is ideal, we can say that the rotational torque developed at the level of the rotating disc is same. Hence, for effective breaking to occur, we provided a retardation torque greater than or equal to that of the rotating disc. Critically examining our results, we can determine that the electromagnetic force or torque is quite greater than the rotational torque of the disc. This therefore provides us with much confidence that the rotating disc can actually come to rest if the retarding force is applied. Notwithstanding, we also have sources of loses, especially joules lost at the level of the electromagnets. A back electromotive force (emf) was produced when the coils were supplied. This back emf is noticeable when switching off

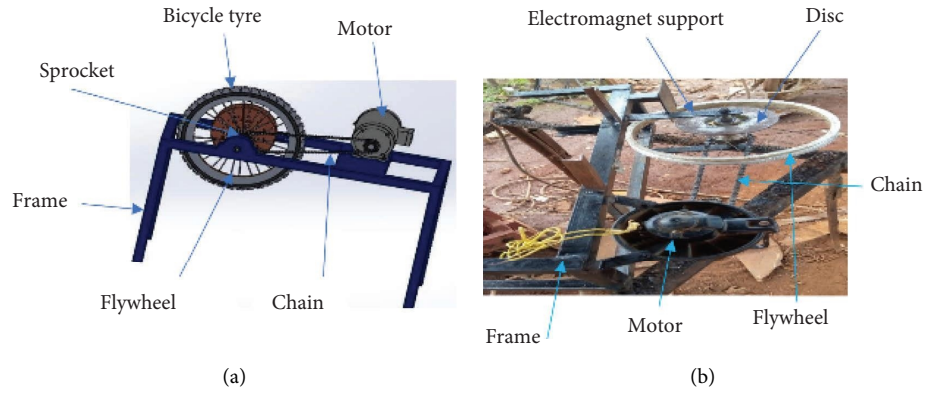

Figure 7: Mechanical realization: (a) SolidWorks design; (b) design model in construction process.

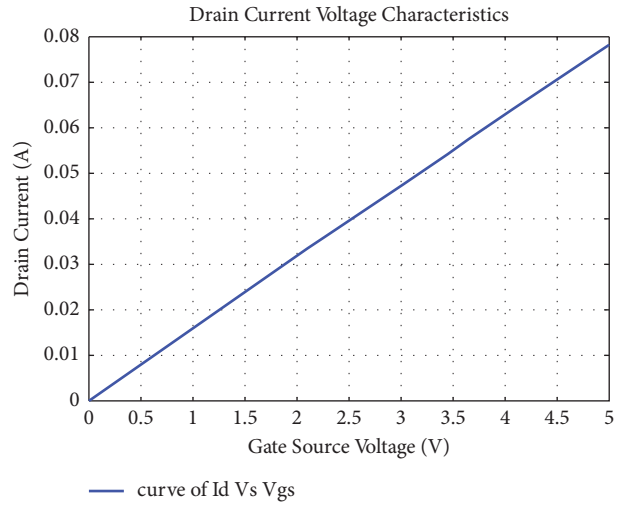

Figure 8: Control voltage.

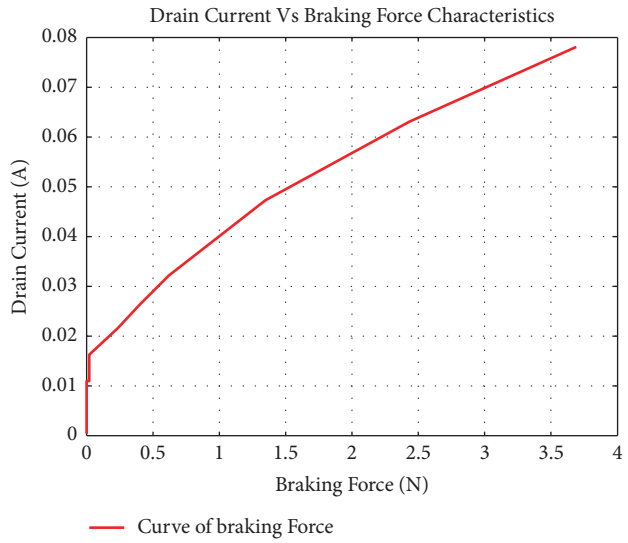

Figure 9: Control electromagnetic force.

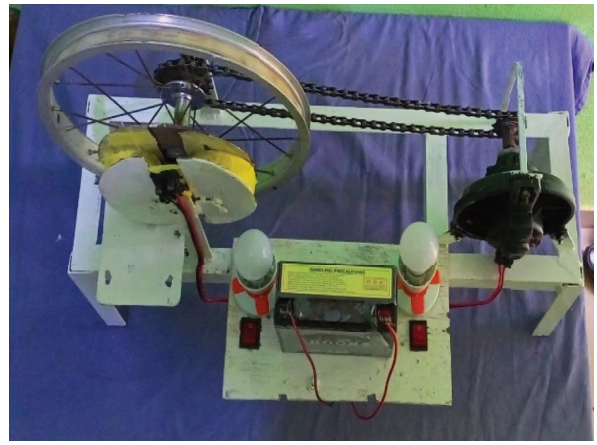

Figure 10: Top view of the proposed system.

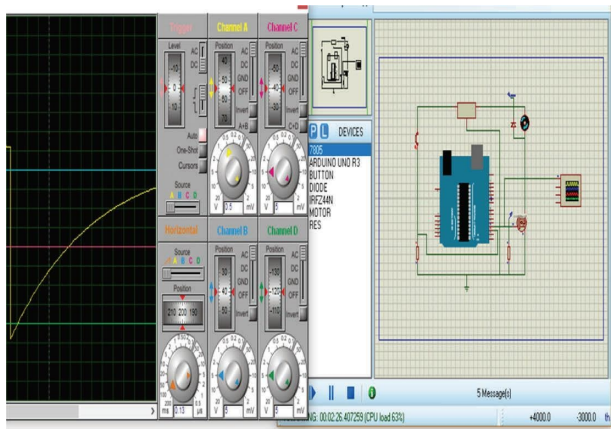

Figure 11: Simulated control drain current.

the electromagnet. However, the current associated with this emf is the eddy current and produces a magnetic field that contributes to the retardation of the disc.

5. Conclusion

In this paper, an electromagnet, mechanical support, and controller are designed and realized to build a contactless breaking system. To build the electromagnet, gauge wires were coiled around a metal core. As the electrical current moves around the loops of the coil, it generates a magnetic field and subsequently a Lorentz force appears as the breaking force. The software SolidWorks 2018 version is used to design the mechanical support. Iron is dimensioned, cut, and welded for the fabrication. The Arduino Uno board and MOSFET help to control the coil currents that generate the breaking force. The variation of the breaking force depends on the PWM signal produced by the microcontroller. All these three system components are put together to achieve a braking system without contact. The built system is able to produce a breaking force growing from zero to 1.43 N within a specified time range of 5 seconds. The numerical and experimental results both show a very good agreement, so we can say that our proposed contactless breaking system can be an efficient solution for industrial machines having sharp blades mounted on moving parts that need to be slow down in a shortest possible time in case they are shutdown to reduce their extreme dangerousness.

Data Availability

No data were used to support this study.

Conflicts of Interest

The authors declare that there are no conflicts of interest regarding the publication of this paper.

Authors' Contributions

All authors contributed to the study conception and design. Tchahou Tchendjeu Achille Ecladore and Yungho Edickson Bobo were responsible for material preparation, data collection, and analysis. Nfah Eustace Mbaka wrote the first draft of the manuscript, and all authors commented on previous versions of the manuscript. All authors were involved in revising the comments given by the editorial board. All authors have read and approved the final manuscript.

References

[1] S. Shenshen, *Automobile Brake System*, Sovonia University of Applied Sciences, Kuopio, Finland, 2016.

[2] M. D. Shujauddin, A. Malge, F. Mohammed, L. R. Nikhi, and P. S. Shreyas, "Design and fabrication of frictionless braking system," *International Journal of Scientific Engineering and Research*, vol. 11, no. 355, pp. 6–363, 2020.

[3] M. R. A. Putra, M. Nizam, D. D. D. P. Tjahjana, M. Aziz, A. R. Prabowo, and R. P. Aditya, "Application of multiple unipolar axial eddy current brakes for lightweight electric vehicle braking," *Applied Sciences*, vol. 10, no. 13, p. 4659, 2020.

[4] F. Arago, *Biographies of Distinguished Scientific Men*, DigiCat, Boston, MA, USA, 2020.

[5] P. Sevvel, K. Nirmal, and M. Mukesh, "Innovative electromagnetic braking system," *International Journal of Science, Research and Development*, vol. 3, no. 46-53, p. 2, 2014.

[6] B. Oriano and M. Chiampi, "Hystereris and eddy current effects in ferroresonant," *LCR circuits" Journal of Magnetism and Magnetic Materials*, vol. 304, p. 2, 2006.

[7] S. kumar and V. Kumar, "Automatic emergency braking system," *International Journal of Renewable and Sustainable Energy*, vol. 1, no. 3, pp. 2394–8299, 2007.

[8] A. Aravind, V. R. Akilesh, S. Gunaseelan, and S. Ganesh, "Eddy current embedded conventional braking system," *International Journal of Institutional Research, Science, Engineering and Technology*, vol. 5, p. 7, 2016.

[9] G. Anantha Krishna and K. Sathish Kumar, "Investigation on eddy current braking systems" A review," *Applied Mechanics and Materials*, vol. 592–594, pp. 1089–1093, 2014.

[10] K. S. Akshay, U. Nagnath, A. Huzaifa, and N. Bhushan, "Enhancement of braking system in automobile using Electromagnetic Braking," *IOSR Journal of Mechanical and Civil Engineering*, vol. 9, 2007.

[11] S. Akash, P. Myron, P. Roger, and I. Yogesh, "Design and development of electromagnetic braking system," *International Research Journal of Engineering and Technology*, vol. 7, no. 10, pp. 1054–1056, 2020.

[12] American Wire Gauge, "Wire gauge and current limits including skin depth and tensile strength," 2023, https://www.powerstream.com/Wire_Size.htm.